



1

## 2 **Supporting Information for**

### 3 **Sensory input to cortex encoded on low-dimensional periphery-correlated subspaces**

4 **Andrea K Barreiro, Antonio J Fontenele, Cheng Ly, Prashant Raju, Shree Hari Gautam, Woodrow L Shew**

5 **Corresponding Author: Woodrow L Shew**

6 **E-mail: [shew@uark.edu](mailto:shew@uark.edu)**

#### 7 **This PDF file includes:**

8     Supporting text

9     Figs. S1 to S2

10    SI References

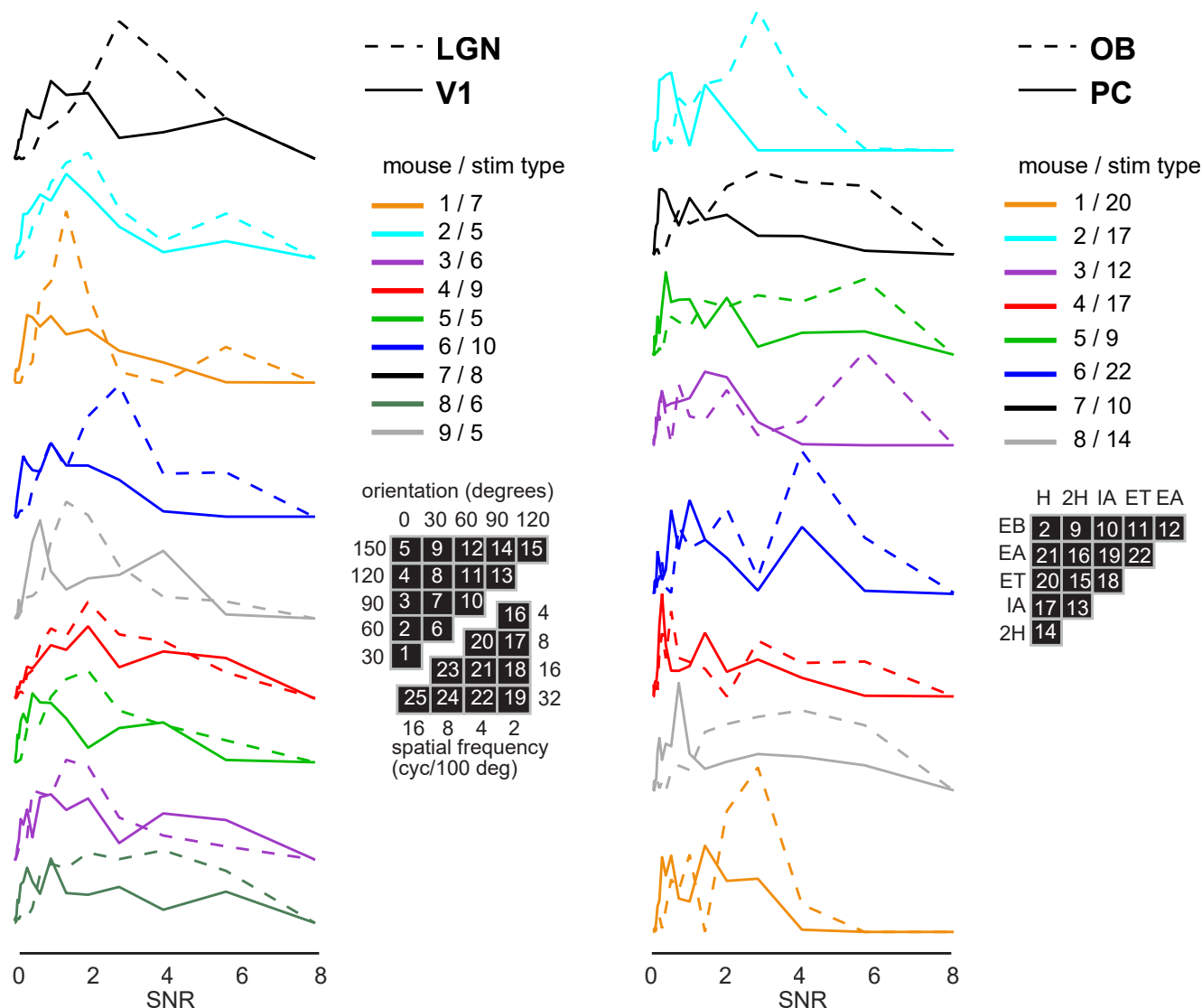


**Fig. S1. Signal-to-noise ratio is lower in cortex than upstream regions.** In the main text, it was suggested that signal-to-noise is lower in primary sensory cortex compared with the upstream regions, closer to the sensory periphery, that provide sensory input to cortex. Here we show quantitatively that this is true for the visual system and olfactory system data that we analyzed. [Left] Each solid line is a distribution of SNR values for the 10000 randomly chosen pairs of V1 neurons analyzed in the main text. Each dashed line is a SNR distribution for the corresponding 10000 pairs of LGN neurons. Here we took the 2x2-population-level SNR to be  $\sqrt{\mu^T \Sigma^{-1} \mu}$ , where  $\mu$  is a two-element vector of response differences (response to stimulus type A minus response to stimulus type B) and  $\Sigma$  is the response covariance matrix for the two neurons. Each color represents an example from a different mouse and a different pair of stimuli. The 'stim type' number in the legend refers to a specific pair of grating orientations or spatial frequencies as labeled in the black grids. [Right] Same as the left, but based on the olfactory system. Note that for both the visual and the olfactory systems, the solid distributions indicate a lower typical SNR in cortex compared to the upstream regions (dashed). Also note that this set of example mice and stimulus types is the same as those shown in Fig 4B,D,F and H, with the same color code.

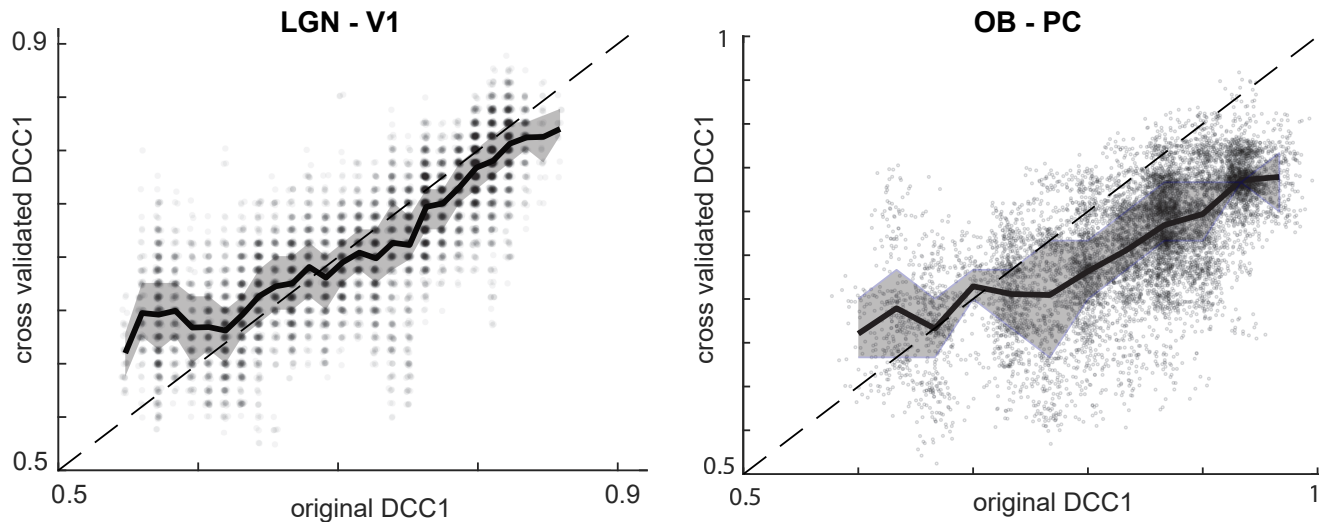


**Fig. S2. Cross-validation of DCC1.** Like many other decoding algorithms, our proposed CC1 decoding can generate artificially high values of decoding accuracy if there are too few stimulus trials or if response dimensionality is too high. In the context of our work, response dimensionality is simply the number of neurons from each population, which was 2 for all the results reported here. Although our theory is not limited to this 2-dimensional case, reliable tests of the theory using a finite number of trials require a low dimensional response. We tried 3x3 populations and found (not shown) that the cross-validated DCC1 became less reliable than shown here. For this reason, we chose to work with 2x2 populations. For our 2x2 populations, we did a 10-fold cross validation to verify that our measured values of DCC1 were reliable. For a given 2x2 population, we used 9/10 of the stimulus trials to calculate CC1 directions and determine the optimal decoding threshold on the CC1-projected responses. Then, we used the same projection and threshold to calculate decoding accuracy for the held out 1/10 of trials. We repeated this for the 10 unique folds of training and hold-out trials and finally averaged the 10 decoding accuracy values across the 10 folds. These averaged decoding accuracies are reported here compared to the original decoding accuracies reported in the main text. Note that the cross validated DCC1 values are strongly correlated with the original values, which means they are reliable. However, it is clear that for the olfactory data (right), which had only 15 trials per stimulus type, original DCC1 is more prone to over estimation compared the cross validated DCC1. The visual system data (left) included 42 trials per stimulus type, which allows a better match between original and cross validated DCC1. The dashed line (slope unity) marks equality between original and cross validated DCC1. Each point represents one of 10000 randomly chosen populations. The dark line and shaded area indicates the median and quartiles of the points, respectively. Points are displayed with 20% opacity, so that density of points is clearer.

## Mathematical Results

**Introduction.** We consider the case of two populations of neurons whose responses to two stimuli, A and B, are correlated both within and across populations. We assume the responses to each stimulus can be described by a multivariate Gaussian, i.e.

$$P(r_X, r_Y|S) = N\left(\begin{bmatrix} \mu_{X,S} \\ \mu_{Y,S} \end{bmatrix}, \Sigma_S\right),$$

where  $S = \{A, B\}$ ,  $\mu_{X,S} \in \mathbb{R}^m$ ,  $\mu_{Y,S} \in \mathbb{R}^n$ , and  $\Sigma_S$  is a symmetric, positive-definite matrix of size  $(m+n) \times (m+n)$ . Here X and Y refer to two populations of neurons which are both responsive to A and B, containing m and n neurons respectively; for example, Y may be a cortical region and X a pre-cortical region which supplies afferent input to Y. Without loss of generality, we simplify notation by shifting the mean responses so that  $\mu_{X,A} = 0$ ,  $\mu_{Y,A} = 0$ ; thus, we can drop the stimulus subscript on the mean vectors and use  $\mu_X = \mu_{X,B}$  and  $\mu_Y = \mu_{Y,B}$ .

We next consider how to decode the stimulus, using only the responses within each population. We assume that the covariance matrix is the same for both stimuli: i.e.  $\Sigma_A = \Sigma_B =: \Sigma$ . In this case the optimal decision boundary is given by a hyperplane in  $\mathbb{R}^m$  or  $\mathbb{R}^n$ ; equivalently, by a one-dimensional projection of the response vector. The decision boundary is given by (for example)  $u \in \mathbb{R}^m$  such that  $u^T \Sigma_X^{-1} \mu_X = \frac{1}{2} \mu_X^T \Sigma_X^{-1} \mu_X + \log \frac{P(B)}{P(A)}$ , (Here,  $\Sigma_X$  and  $\Sigma_Y$  are the marginal covariances in populations X and Y respectively.) Therefore, the projection vector must be the normal vector to this plane; i.e.:

$$v_X = \Sigma_X^{-1} \mu_X, \quad v_Y = \Sigma_Y^{-1} \mu_Y \quad [1]$$

in populations X and Y respectively. Alternatively, observing that  $v^T r_X|S$  is a one-dimensional Gaussian with

$$\mathbb{E}[v^T r_X|S] = v^T \mu_{X,S}, \quad \text{Var}[v^T r_X|S] = v^T \Sigma v, \quad [2]$$

we can derive the same outcome by maximizing the signal-to-noise ratio; i.e.  $v_X = \text{argmin} \left( \frac{\sqrt{v^T \Sigma v}}{v^T \mu_X} \right)$ . From the perspective of *linear discriminant analysis*, this maximizes between-class (where “class”=stimulus identity) variability while minimizing within-class variability (1).

**When cross-region noise correlations are absent, CC1 is a perfect decoder.** We now compute the projection directions associated with canonical correlation analysis (CCA). Given two sets of zero-mean observations from X and Y, the goal of CCA is to find the linear projections of the observations that are maximally correlated (2). This technique uses the full stimulus-averaged population response; however, we will show that under certain conditions, the maximally correlated direction from CCA coincides with the optimal decoder. Assuming  $P(A) = P(B)$ , the covariance structure within each population is

$$\Sigma_{XX} = \frac{1}{4} \mu_X \mu_X^T + \Sigma_X; \quad \Sigma_{YY} = \frac{1}{4} \mu_Y \mu_Y^T + \Sigma_Y$$

while the stimulus-averaged covariance matrix between populations X and Y is

$$\Sigma_{XY} = \frac{1}{4} \mu_X \mu_Y^T + \Sigma_C \quad [3]$$

Here  $\Sigma_X$ ,  $\Sigma_Y$ , and  $\Sigma_C$  are the covariances within and across-populations: i.e.

$$\Sigma = \begin{bmatrix} \Sigma_X & \Sigma_C \\ \Sigma_C^T & \Sigma_Y \end{bmatrix}$$

We now seek to find the directions which maximize correlation across the population; that is

$$R_{CC1} = \max_{\mathbf{a}, \mathbf{b}} \frac{\mathbf{a}^T \Sigma_{XY} \mathbf{b}}{\sqrt{\mathbf{a}^T \Sigma_{XX} \mathbf{a}} \sqrt{\mathbf{b}^T \Sigma_{YY} \mathbf{b}}}$$

We denote the vectors that achieve this maximum as  $v_{X,CC1}$  and  $v_{Y,CC1}$  respectively; i.e.

$$v_{X,CC1}, v_{Y,CC1} = \text{argmax}_{\mathbf{a}, \mathbf{b}} \frac{\mathbf{a}^T \Sigma_{XY} \mathbf{b}}{\sqrt{\mathbf{a}^T \Sigma_{XX} \mathbf{a}} \sqrt{\mathbf{b}^T \Sigma_{YY} \mathbf{b}}}$$

The vectors  $v_{X,CC1}$  and  $v_{Y,CC1}$  can be obtained by finding the principal eigenvectors of  $D_X$  and  $D_Y$  respectively:

$$D_X = \Sigma_{XX}^{-1} \Sigma_{XY} \Sigma_{YY}^{-1} \Sigma_{XY}^T; \quad D_Y = \Sigma_{YY}^{-1} \Sigma_{XY}^T \Sigma_{XX}^{-1} \Sigma_{XY} \quad [4]$$

and the corresponding eigenvalue is the correlation ( $R_{CC1}$ ) squared: that is,

$$D_X v_{X,CC1} = \lambda v_{X,CC1} \Leftrightarrow R_{CC1} = \sqrt{\lambda}$$

We note that the cross-covariance matrix  $\Sigma_{XY}$  has two contributions, one reflecting signal correlations ( $\frac{1}{4} \mu_X \mu_Y^T$ ) and the other noise correlations ( $\Sigma_C$ ). The latter reflects trial-to-trial correlations which are not reflected in the mean response. We will now show that when noise correlations are absent ( $\Sigma_C = 0$ ), the principal CCA direction coincides with the optimal decoding direction. Without loss of generality, we focus on  $D_X$ ; parallel statements hold for  $D_Y$ .

**Lemma 1:** If  $\Sigma_C = 0$ , then  $D_X$  is a rank 1 matrix.

46 *Proof.* It is well known that the rank of a matrix product is bounded above by the minimum rank of the matrices; i.e.  
 47  $\text{rank}(AB) \leq \min(\text{rank}(A), \text{rank}(B))$ . From Eq. (3)  $\Sigma_{XY}$  is the sum of two matrices, the first of which is rank 1; if  $\Sigma_C = 0$ ,  
 48 therefore, the sum is rank 1 as well. Therefore any matrix product that includes  $\Sigma_{XY}$  has rank at most 1.  $\square$

49 **Theorem 1:** If  $\Sigma_C = 0$ , then the correlated (non-zero) eigenvector of  $D_X$  coincides with the projection direction which is  
 50 optimal for decoding.  
 51

52 *Proof.* Recall that Eq. (1) shows that  $v_X \propto \Sigma_X^{-1} \mu_X$ . We will show that  $v_X$  is also an eigenvector of  $D_X$ .

53 Consider the formula for  $D_X$ :

$$54 \quad D_X = \Sigma_{XX}^{-1} \Sigma_{XY} \Sigma_{YY}^{-1} \Sigma_{XY}^T$$

55 The cross-population correlation matrix  $\Sigma_{XY}$  is rank 1 and  $\text{range}(\Sigma_{XY}) = \text{Span}\{\mu_X\}$ . Therefore,  $\text{range}(D_X) = \text{Span}\{\Sigma_{XX}^{-1} \mu_X\}$ .

56 Next, we write  $\Sigma_{XX}^{-1}$  in terms of  $\Sigma_X^{-1}$ . Using the matrix determinant lemma, and noting that

$$57 \quad \Sigma_{XX} = \Sigma_X + \mathbf{u} \mathbf{u}^T$$

where  $\mathbf{u} = \mu_X/2$ ,

$$\Sigma_{XX}^{-1} = \Sigma_X^{-1} - \frac{\Sigma_X^{-1} \mathbf{u} \mathbf{u}^T \Sigma_X^{-1}}{1 + \mathbf{u}^T \Sigma_X^{-1} \mathbf{u}} \quad [5]$$

$$= \Sigma_X^{-1} - \Sigma_X^{-1} \mathbf{u} \left( \frac{\mathbf{u}^T \Sigma_X^{-1}}{1 + \mathbf{u}^T \Sigma_X^{-1} \mathbf{u}} \right) \quad [6]$$

58 The second term *already* maps into  $\text{Span}\{\Sigma_X^{-1} \mu_X\}$ , regardless of what vector is multiplied on the right. In conclusion,  
 59  $\text{range}(D_X) = \text{Span}\{\Sigma_X^{-1} \mu_X\}$ ; i.e.  $D_X v_X \propto v_X$ .  $\square$

By using Eq. (6) (and the analogous simplification for  $\Sigma_{YY}^{-1}$ ), one can confirm that the corresponding eigenvalue is

$$\lambda = \left( \frac{s_X^2}{4 + s_X^2} \right) \left( \frac{s_Y^2}{4 + s_Y^2} \right) \quad [7]$$

60 where  $s_X = \sqrt{\mu_X^T \Sigma_X^{-1} \mu_X}$  and  $s_Y = \sqrt{\mu_Y^T \Sigma_Y^{-1} \mu_Y}$  are the signal-to-noise ratios for the  $X$  and  $Y$  populations respectively.  
 61

62 **Theorem 2:** If  $\Sigma_C = 0$ , then any other eigenvector of  $D_X$  gives chance-level decoding.

63 *Proof.* If  $\mathbf{v}^T \mu_X = 0$ , then  $\Sigma_{XY}^T \mathbf{v} = 0$  and therefore  $D_X \mathbf{v} = 0$ . Therefore  $\mathbf{v}$  is an eigenvector of  $D_X$  with eigenvalue 0. But then

$$64 \quad E[\mathbf{v}^T r_X | A] = E[\mathbf{v}^T r_X | B] = 0$$

65 i.e. the stimuli A and B cannot be discriminated.  $\square$

## 66 References

- 67 1. J Cunningham, Z Ghahramani, Linear dimensionality reduction: Survey, insights, and generalizations. *J. Mach. Learn. Res.*  
 68 **16**, 2859–2900 (2015).
- 69 2. H Hotelling, Relations between two sets of variates. *Biometrika* **28**, 321–377 (1936).